



# Photocatalytic treatment of indoor air: Optimization of 2-propanol removal using a response surface methodology (RSM)

Daniel Vildoza<sup>\*</sup>, Corinne Ferronato, Mohamad Sleiman, Jean-Marc Chovelon

Université of Lyon 1, UMR CNRS 5256, Institut de recherches sur la catalyse et l'environnement de Lyon (IRCELYON), 2 Avenue Albert Einstein, F-69626 Villeurbanne, France

## ARTICLE INFO

### Article history:

Received 6 October 2009

Received in revised form 20 November 2009

Accepted 30 November 2009

### Keywords:

Photocatalysis

TiO<sub>2</sub>

2-Propanol

Indoor air

RSM

## ABSTRACT

This paper presents an experimental design methodology for the optimization of the photocatalytic removal of 2-propanol also called isopropyl alcohol (IPA) at indoor air concentration level (ppbv). The response surface methodology (RSM) for the modelization and optimization of the photodegradation of 2-propanol in the presence of titanium dioxide was used. The effect of four different process parameters on the yield of 2-propanol mineralization was determined. Experiments were performed using an annular flow-through reactor with TiO<sub>2</sub> as photocatalyst, 2-propanol as a volatile organic compound (VOC) model, under different ranges of relative humidity (RH: 0–60%), inlet concentration (100–700 ppbv) and flow rate (100–500 mL min<sup>−1</sup>), TiO<sub>2</sub> loading (5–20 g m<sup>−2</sup>). Analysis of reaction intermediates was conducted using an automated thermal desorption technique coupled with gas chromatography–mass spectrometry (ATD–GC–MS) whereas a gas chromatograph equipped with a pulsed discharge helium photoionization detector (GC–PDHID) was used for on-line measurements of CO and CO<sub>2</sub> at ppbv level. RH was found as the principal parameter that affect significantly the mineralization and the formation of acetone, the principal reaction intermediate from the photocatalytic oxidation of 2-propanol. For example an immediate and total removal of 2-propanol at very low % of RH along with a high rate of mineralization without any by-products was found. Many strong interactions between the parameters were also found ([2-propanol]–flow rate, RH–[TiO<sub>2</sub>], [2-propanol]–RH). The model obtained ( $R^2 = 0.9965$ ) shows a satisfactory correlation between the values of experimental data and predicted values of 2-propanol mineralization (CO<sub>2</sub>).

© 2009 Elsevier B.V. All rights reserved.

## 1. Introduction

Photocatalytic oxidation (PCO) is becoming more and more attractive today because indoor air pollution has come to be recognized as a serious problem that needs to be addressed immediately. The increasing interest in PCO in air treatment showed by the industry and researchers can be demonstrated recently by the growing number of scientific publications and the commercialization of different TiO<sub>2</sub>-based photocatalytic products (air cleaners, air purification materials) [1–3]. However several unanswered issues are still present like the difficulty to find a standardization method to evaluate and optimize PCO in indoor air treatment.

PCO uses photons with energy greater than the band gap of a semiconductor to promote valence electrons to the conduction band and thus forming electrons and holes to initiate oxidation–reduction reactions [4]. The free reactive radicals formed at the surface of semiconductor oxidize and destroy VOCs. PCO, rather

than adsorbing VOCs on adsorbent such as active carbon, oxidizes VOCs to CO<sub>2</sub> and H<sub>2</sub>O. However the performance of PCO on VOCs depends of many operational parameters that may affect some partially oxidized by-products [5]. The removal efficiencies of PCO for most indoor VOCs are relatively high and the production of by-products is relatively low [6,7].

In conventional approach, optimization is usually carried out by varying one variable a time while keeping all other variables fixed at a specific set of conditions. It is not only time-consuming, but also usually incapable of reaching the true optimum due to ignoring the eventual interactions among variables [8]. On the other hand, the response surface methodology (RSM) has been proposed to determine the influences of individual factors and their interactive influences. The RSM is a statistical technique for designing experiments, building models, evaluating the effects of several factors, and searching optimum conditions for desirable responses. With RSM, the interactions of possible influencing parameters on treatment efficiency can be evaluated with a limited number of planned experiments [9].

Several works have proved that RSM is a powerful statistical tool for optimization of photocatalytic oxidation processes; however most of these studies were focused on water applications

<sup>\*</sup> Corresponding author. Tel.: +33 4 72 44 58 52; fax: +33 4 72 44 53 99.

E-mail address: [daniel.vildoza@ircelyon.univ-lyon1.fr](mailto:daniel.vildoza@ircelyon.univ-lyon1.fr) (D. Vildoza).

[10–15]. As far as we are concerned, no scientific work has been published dealing with the application of RSM to PCO in indoor air treatment. Moreover, many documented air studies have primarily dealt with high parts per million (ppmv) concentrations, which is more typical for chemical process stream concentrations than indoor air quality concentrations (ppbv). Extrapolation of oxidation performance data collected at concentrations much higher than those in the intended application may not be valid in PCO of VOCs [16].

2-Propanol also called isopropyl alcohol (IPA) was chosen as a model reactant because this molecule was reported in the top indoor air pollutants based on measurements at indoor locations [17,18] and also was reported in different modes of public transportation [7]. PCO of 2-propanol is a good VOC model because the initial reaction pathway involves almost exclusively the partial oxidation to acetone [19].

The present work presents an experimental approach combining advanced analytical methods and response surface methodology for the PCO study of 2-propanol. For the quantification and identification of the organic gas phase reaction products, an automated thermal desorption technique coupled with gas chromatography–mass spectrometry (ATD–GC–MS) was used. For the evaluation of the mineralization performance of PCO process, a gas chromatograph equipped with a pulsed discharge helium photoionization detector (GC–PDHID) at ppbv levels was adjusted. For the modelization, optimization and the study of the influence of different parameters such as 2-propanol inlet concentration, relative humidity, flow rate,  $\text{TiO}_2$  loading in the PCO of 2-propanol an experimental design based in RSM was used.

## 2. Experimental

### 2.1. Reactor and experimental set-up

Fig. 1 shows a schematic representation of the experimental set-up used for the PCO of 2-propanol in gas phase. Experiments were conducted in continuous flow mode using an annular flow-through reactor of about 50 mL, made of stainless steel and equipped with an optical Pyrex glass window (transmittance: wavelength  $>290$  nm), a water cell to avoid heating and a high

pressure mercury UV lamp (HPK 125 W, Philips). The photocatalytic medium was non-woven paper (natural cellulose fiber), coated with  $\text{TiO}_2$  PC-500 (100% anatase, BET area:  $300 \text{ m}^2 \text{ g}^{-1}$ , crystal size: 5–10 nm) supplied by Ahlstrom, France.

A gaseous stream of 2-propanol was generated using a permeation tube from Calibrage (France) filled by pure liquid 2-propanol and placed inside a furnace maintained at a constant temperature of  $50^\circ\text{C}$ . A He gas at a constant flow rate of  $50 \text{ mL min}^{-1}$  was passed over permeation tube and subsequently mixed with  $\text{O}_2$  or He and water vapour ( $\text{H}_2\text{O}$ ) at gas flow rates corresponding to target 2-propanol concentration ranging from 100 to 700 ppbv. The gas flow rates were adjusted using mass flow controllers in the  $0$ – $1000 \text{ mL min}^{-1}$  range (Brooks, 5850S series). The final gas stream humidity and temperature were measured using a thermohygrometer (Rotronic Hygropalm 1, France).

### 2.2. Sampling and analysis of gaseous intermediates

During the irradiation experiments, 2-propanol and gas phase reaction intermediates were collected for 2–30 min at regular time intervals and at flow rate of  $30 \text{ mL min}^{-1}$  using multibed solid sorbent tubes packed with Carbotrap C, Carbotrap B and Carbosieve III (Supelco) in that order. In preliminary experiments, the sampling conditions were tested against breakthrough by collecting a 900 mL sample of 2-propanol and the potential degradation intermediates with two identical tubes connected in series. The analysis showed no breakthrough from the first trap to the second one, confirming that no loss of products occurs during the sampling step. On the other hand, the repeatability of the whole analytical procedure (sampling and analysis) was measured with a series of 5 samples of standards and the resulting relative standard deviation was  $<2\%$ . Analysis was carried out using a GC–MS (Clarus 500, Perkin Elmer), equipped with an automated thermal desorption unit (Turbomatrix, Perkin Elmer). MS identification was conducted (i) by comparing the retention times and mass spectra to available authentic standards, (ii) by using the NIST library with a fit higher than 90%. An effort was also made to quantify the reaction intermediate present in gas phase (acetone) in order to determine the main reaction route and to better understand the reaction mechanism. All analytes were quantified

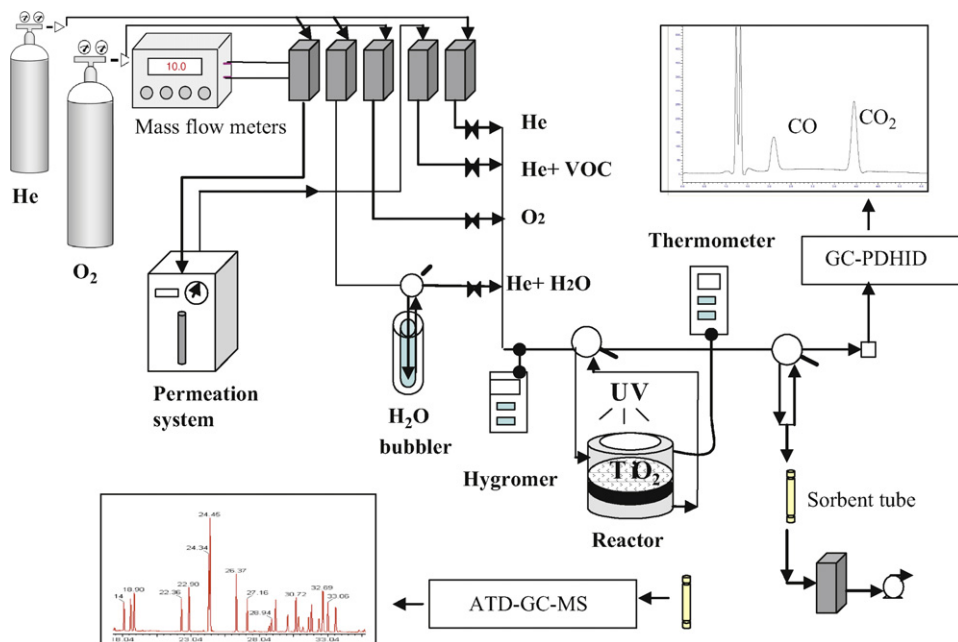


Fig. 1. Schematic representation of the experimental set-up used for the PCO of 2-propanol.

using ATD–GC–MS multipoint calibration curves developed from pure chemical standards, purchased from Aldrich.

### 2.3. On-line measurements of CO/CO<sub>2</sub>

The formation of CO/CO<sub>2</sub> during the reaction was monitored every 1 h using a GC–PDHID instrument [20,21] that consisted of: (i) one 10-way Valco valves (V10) equipped with a 1 mL sample loop, (ii) two packed chromatographic columns placed in parallel configuration: a Porapak Q (L: 5 m, ID: 1/8") and a Tamis 13-X (L: 2 m, ID: 1/16") from RESTEK, (iii) a PD-D3-I detector (Valco instruments). Carrier gas was ultra pure He N60 from Air liquide (99.99999% purity) which was additionally purified by a Valco HP-2 purifier. Oven temperature was 45 °C and columns flow rates were 12 mL min<sup>-1</sup> for Tamis 13-X and 20 mL min<sup>-1</sup> for Porapak Q. Using these conditions, analysis time was around 5 min. Calibration of CO/CO<sub>2</sub> was carried out using a standard mixture of CO/CO<sub>2</sub> (5 ppmv in He). The detection limits for CO and CO<sub>2</sub> were 40 and 20 ppbv respectively, with a relative standard deviation of 0.2% for CO<sub>2</sub> and 0.8% for CO.

### 2.4. Experimental design data analysis

The chemometric approach was performed using a central composite design (CDD). Analysis of the experimental data was supported by the statistical graphics software system. "Design expert"(version 7.6.1) software was used for regression and graphical analyses of the obtained data.

## 3. Results and discussion

### 3.1. Preliminary experiments

#### 3.1.1. Photocatalyst media pre-treatment

A series of experiments was conducted to evaluate the photocatalyst medium to insure an efficient elimination of adsorbed contaminants on the surface before the PCO treatment of 2-propanol. For this purpose the TiO<sub>2</sub> media was pre-treated by UV irradiation without 2-propanol just with pure oxygen/He (2/98 v/v), at gas flow (100 mL min<sup>-1</sup>) with and without RH. Fig. 2 shows the formation of CO<sub>2</sub> after 20 h of pre-treatment of the TiO<sub>2</sub> media using different percentages of relative humidity and with different concentrations of TiO<sub>2</sub>. The results showed also an effect in the presence of relative humidity on the CO<sub>2</sub> generation from the TiO<sub>2</sub> media irradiation. In the absence of humidity after 20 h of

irradiation, the amount of CO<sub>2</sub> generated from TiO<sub>2</sub> media was stable at 100 ppbv of CO<sub>2</sub> at different TiO<sub>2</sub> loadings (5–20 g m<sup>-2</sup>). However in the presence of humidity, the CO<sub>2</sub> generated from the TiO<sub>2</sub> media irradiation was stable at 1000 ppbv at the different percentages of RH (40–60%) after 20 h in both concentrations of TiO<sub>2</sub> (5–20 g m<sup>-2</sup>).

Therefore more experiments were realized to verify the cause of CO<sub>2</sub> generation from TiO<sub>2</sub> media. The TiO<sub>2</sub> media was also irradiated until 48 h at different conditions (0–60% RH) with no changes in the values of CO<sub>2</sub> obtained after 20 h of irradiation. Therefore 24 h was chosen as the pre-treatment time irradiation for the TiO<sub>2</sub> media before the experiments of PCO of 2-propanol.

The commercial photocatalytic media used in this study is made of cellulose fibers. It is well known that cellulose is sensitive to UV irradiation and can be degraded by photocatalysis [22]. It is possible that the coverage of photoinactive silica used to bind TiO<sub>2</sub> to the cellulose fiber is not perfect and there is a contact between the TiO<sub>2</sub> and the cellulose. It can be concluded that the CO<sub>2</sub> found in the pre-treatment experiments comes from the degradation of the natural cellulose fiber from the TiO<sub>2</sub> Ahlstrom support during the UV irradiation. These results show the importance of previous photocatalytic media treatment before PCO degradation especially for low VOCs concentration studies (ppbv).

#### 3.1.2. Choice of factors and responses

PCO for in indoor air purification can be affected by a large number of parameters such as TiO<sub>2</sub> loading (1), inlet VOC concentration (2), light intensity (3), oxygen concentration (4), flow rate (5), humidity (6), etc. Therefore preliminary experiments were conducted to detect the variables having the most impact on the PCO of 2-propanol performance (mineralization, conversion). Among the six parameters investigated (1–6) it was found that the main factors were TiO<sub>2</sub> loading, inlet 2-propanol concentration, flow rate and humidity. The remaining parameters such as O<sub>2</sub> and light intensity in the range studied (1–10% v/v and 2–6 mW cm<sup>-2</sup>, respectively) were found to be less important, probably because of the low concentration of the target pollutant, therefore they were not considered as variables in the experimental design. There values were kept constant during all the experiments (O<sub>2</sub>: 2% v/v, light intensity: 3.2 mW cm<sup>-2</sup>).

The experimental measured responses (*R*) during the all experimental design were: mineralization (*R*<sub>1</sub>), 2-propanol conversion (*R*<sub>2</sub>) and selectivity of acetone (*R*<sub>3</sub>). The mineralization was determined from the online analysis of CO<sub>2</sub> performed by GC–PDHID. Previous experiments were performed for monitoring the CO<sub>2</sub> formation during 48 h of 2-propanol degradation at different conditions. It was noted a stability in CO<sub>2</sub> formation after 2 h of degradation. In this context, to be sure of the CO<sub>2</sub> stability, 6 h was chosen as experimental time for all the experimental design.

The mineralization was calculated by comparing the concentration of carbon dioxide (CO<sub>2</sub>) produced to the theoretical one using the following equation:

$$\text{Mineralization (\%)} = \frac{[\text{CO}_2]_{\text{measured}}}{3 \left[ [\text{2-propanol}]_{\text{in}} - [\text{2-propanol}]_{\text{out}} \right]} \times 100 \quad (1)$$

2-propanol conversion and selectivity of acetone were also measured in the experimental design by ATD–GC–MS. The conversion of 2-propanol (*X*<sub>2-propanol</sub>) was calculated from the difference between the inlet and outlet 2-propanol concentrations, as:

$$X_{2\text{-propanol}} = \frac{[\text{2-propanol}]_{\text{in}} - [\text{2-propanol}]_{\text{out}}}{[\text{2-propanol}]_{\text{in}}} \quad (2)$$

$$\text{Conversion (\%)} = X_{2\text{-propanol}} \times 100 \quad (3)$$

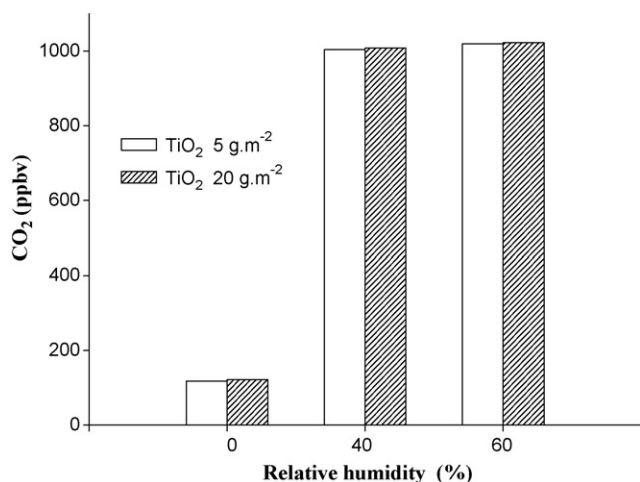


Fig. 2. Effect of the humidity on the CO<sub>2</sub> generation during the UV pre-treatment of different support loadings after 20 h.

**Table 1**

Independent variables and their levels for the central composite design used in the present study.

Variable	Symbol	Coded levels		
		Low (−1)	Center (0)	High (+1)
2-Propanol (ppbv)	A	100	400	700
Relative humidity (%)	B	0	30	60
Flow rate (mL min <sup>−1</sup> )	C	100	300	500
TiO <sub>2</sub> (g m <sup>−2</sup> )	D	5	9	20

The selectivity of acetone ( $S_{\text{acetone}}$ ) was determined by comparing the concentration of acetone from the PCO of 2-propanol and the concentration of 2-propanol converted:

$$S_{\text{acetone}} = \frac{[\text{Acetone}]}{[\text{2-propanol}]_{\text{initial}} X_{\text{2-propanol}}} \quad (4)$$

### 3.2. Experimental design methodology

#### 3.2.1. Central composite design

In this present study, central composite design (CCD) which is a widely used form of RSM, was employed for the optimization of PCO treatment of 2-propanol at indoor air levels. It is an effective design that is ideal for sequential experimentation and allows a reasonable amount of information for testing lack of fit while not involving an unusually large number of design points [23]. 2-Propanol inlet concentration, relative humidity, flow rate and TiO<sub>2</sub> loading were considered as the independent, process-specific variables, while percentage of mineralization, 2-propanol conversion,  $S_{\text{acetone}}$  were considered as the dependent variable (response). The four independent variables were converted to dimensionless ones (A, B, C, D), with the coded values at levels: −1, 0, +1. Values of the independent variables and their variation limits were

$$\begin{aligned} \text{Mineralization (\%)} = & 77.1 - 15.0[\text{2-propanol}] - 32.2\text{RH} - 7.5\text{flow rate} + 11.0[\text{TiO}_2] \\ & - 4.3[\text{2-propanol}]\text{flow rate} + 5.5\text{RH}[\text{TiO}_2] - 12.9\text{RH}^2 - 10.9\text{flow rate}^2 \\ & - 12.3[\text{2-propanol}]^2[\text{TiO}_2] + 12.9[\text{2-propanol}]\text{RH}^2 \end{aligned} \quad (5)$$

determined basing on the results obtained in preliminary studies and are presented in Table 1.

A four-factorial, three level CCD consisting of 26 experimental runs was performed in the present work, including two replications at the center point. The complete experimental design matrix and the responses based on experimental runs proposed by CCD for the PCO 2-propanol treatment are given in Table 2.

Furthermore, in a previous study [24,25], we have shown that the conversion and mineralization behaviors are completely different. 2-Propanol conversion response ( $R_2$ ) shows high values (%) in all the experimental runs which does not imply an optimum performance of PCO because of the different values obtained in the mineralization response ( $R_1$ ) as shown in Table 2. This means that the performance of PCO could not be evaluated based only on the conversion values of a specific pollutant. Acetone selectivity ( $R_3$ ) was present only in the experimental runs with high levels of RH.

As the main goal of the PCO indoor air treatment is to achieve to a complete mineralization (CO<sub>2</sub>) of the pollutant and because of the lack of information of mineralization at low VOCs concentrations (ppbv) in the literature, the percentage of mineralization ( $R_1$ ) was elected for the modelization and optimization with RSM analysis for the experimental design.

A semi-empirical expression in Eq. (5) consisting in 11 statistically significant coefficients were obtained from the data

**Table 2**

Experimental design matrix and responses based on experimental runs proposed by CCD design.

Run	Independent variables				Response (R)		
	A	B	C	D	Experimental		
	[2-propanol] (ppbv)	RH (%)	Flow rate (mL min <sup>−1</sup> )	[TiO <sub>2</sub> ] (g m <sup>−2</sup> )	$R_1$	$R_2$	$R_3$
1	700	60	100	20	35	99	0.18
2	400	60	300	9	32	100	0
3	700	0	500	5	78	98	0
4	700	30	300	9	61	100	0
5	100	60	500	5	15	94	0.60
6	400	0	300	9	96	100	0
7	100	0	500	5	92	100	0
8	400	30	300	20	89	100	0
9	100	60	100	5	21	99	0.53
10	100	0	100	20	82	97	0
11	100	30	300	9	91	100	0
12	400	30	500	9	59	100	0.15
13	700	60	500	20	12	98	0.36
14	700	0	100	20	90	95	0
15	400	30	300	9	78	100	0
16	100	60	100	20	32	96	0.62
17	700	0	100	5	100	99	0
18	100	0	100	5	100	99	0
19	400	30	300	5	67	100	0.10
20	700	0	500	20	65	99	0
21	400	30	100	9	72	100	0
22	100	0	500	20	80	97	0
23	400	30	300	9	78	100	0
24	700	60	100	5	28	99	0.61
25	100	60	500	20	22	95	0.60
26	700	60	500	5	4	91	0.58

$R_1$ : mineralization (%),  $R_2$ : conversion (%),  $R_3$ : acetone selectivity.

analysis using statistical graphics Design-Expert 7.1.6 software at 95% confidence level ( $p < 0.05$ )

This model explains perfectly the experimental range studied ( $R^2$  adjusted = 0.9965). This can be seen in Fig. 3 by comparing the measured values against the predicted responses by the model for the percentage of mineralization of 2-propanol.

#### 3.2.2. Standardized Pareto Chart

To visualize the importance of the calculated factors in Eq. (5), Fig. 4 presents the single factor and the interaction factors depicted in rank order in the form of Pareto Chart. All the standardized factors were in the absolute values and surpass the vertical significance line (95 confidence intervals) which exerts a statistically significant influence on the response. The signs + and − represent positive and negative effects, respectively. Positive effect indicates that percentage of mineralization increases in the presence of high levels of the respective variables within the range studied, while negative effect indicates that mineralization increases in the presence of low levels. Positive quadratic or third order polynomial coefficients indicate a synergistic effect, while negative coefficients indicate an antagonistic effect between or among the variables.

As it can be seen, the most important parameter for the PCO 2-propanol treatment is the relative humidity (B), followed by flow rate (C) and with less importance among the four single parameters, based on 95% significance, the inlet 2-propanol concentration (A) and TiO<sub>2</sub> loading (D). The mineralization of 2-

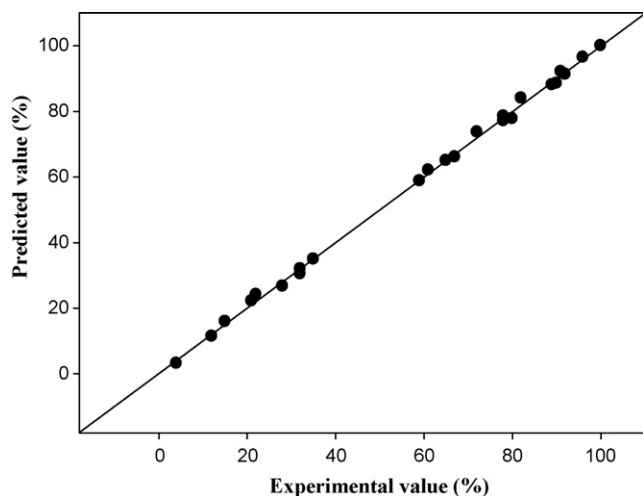


**Fig. 3.** The experimental values plotted against the predicted values derived from the model of mineralization (%) from the experimental design.

propanol was also affected by several interrelated variables such as two factor interactions (BB, BD, CC, AC) and even three factor interactions (ABB, AAD).

### 3.3. Screening of main effects

The influence of all the single factors and interactions of two factors were considered and drawn wherein the lines indicate the

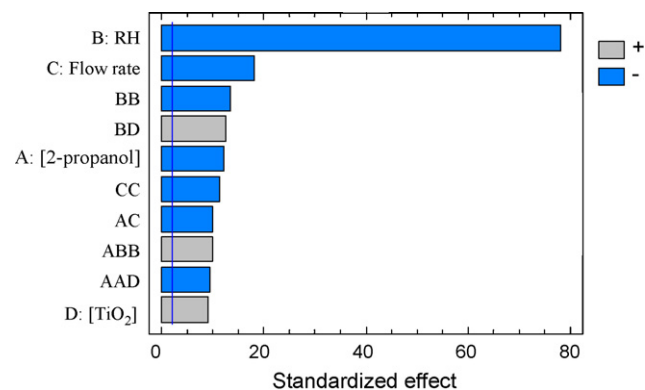


**Fig. 4.** Standardized effects of single and interaction factors on 2-propanol mineralization.

estimated change in response (mineralization %) as each factor is moved from its low level to its high level. Fig. 5 shows the influence of single factors while maintaining all other factors constant at midway value codified as value 0, between their low and high values.

#### 3.3.1. Effect of inlet 2-propanol concentration

It can be seen in Fig. 5a that the variation of the mineralization is linear as a function of the concentration and no quadratic effect is associated with it. We note that inlet concentrations exert a significant influence in the mineralization of 2-propanol especially in the presence of humidity. In the range of 2-propanol

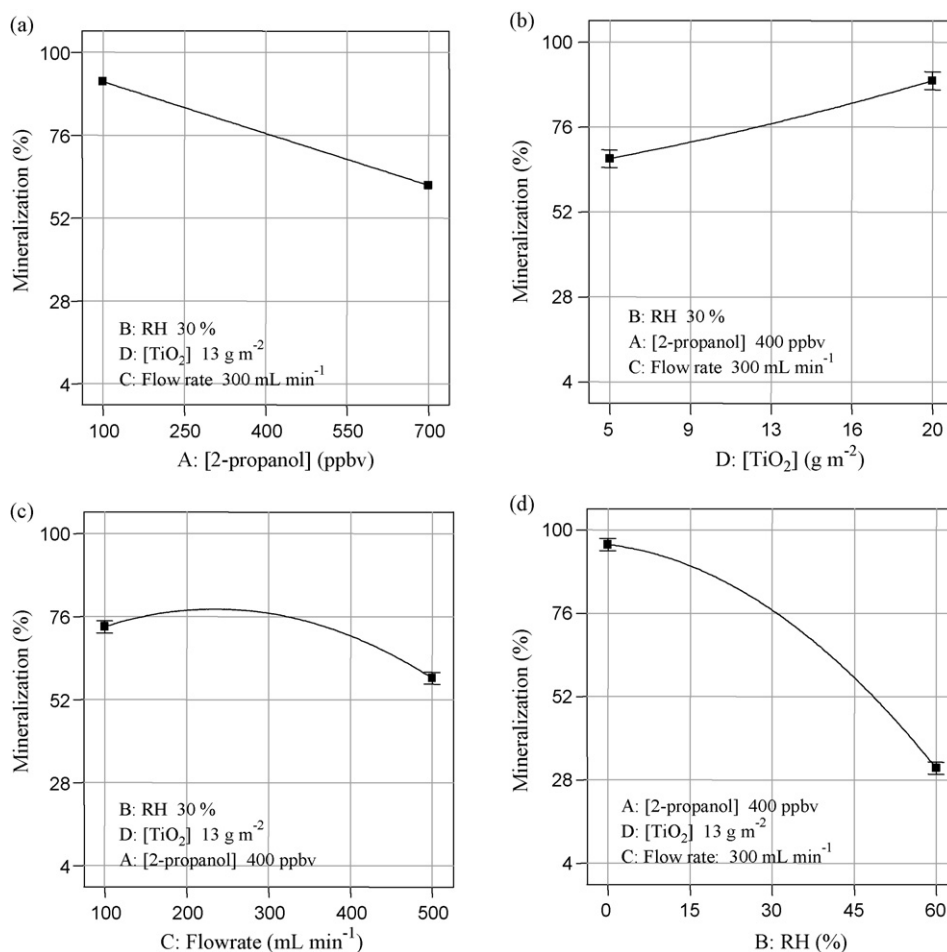


**Fig. 5.** Graphical presentation of the statistical evaluation of the effects of individual factors on the PCO of 2-propanol.



concentration studied (100–700 ppbv) we cannot find an effect of the inlet 2-propanol concentrations at 0% RH, obtaining always very high % of mineralization (fig. not showed). This indicates: (i) the PCO of 2-propanol is not limited by the number of active sites on TiO<sub>2</sub> in the absence of water; (ii) no competitive adsorption effect between by-products and the 2-propanol at ppbv levels is observed, which is not the case of high ppmv range concentrations where saturation and adsorption competition is usually noticed [26,27]. This is why PCO is interesting for VOCs removal at indoor air levels.

### 3.3.2. Effect of TiO<sub>2</sub> loading

As expected TiO<sub>2</sub> loading is a factor with a positive effect of the increased number of TiO<sub>2</sub> active sites during the photocatalytic degradation. The individual effect is shown in Fig. 5b. At RH = 30% we note an increase in the mineralization from 66% to 88% with 5 to 20 g m<sup>-2</sup> of TiO<sub>2</sub>, respectively. As the amount of TiO<sub>2</sub> increased, the mineralization increased proportionally due to a higher surface area of TiO<sub>2</sub>. However, as shown previously in Fig. 4 among the four parameters studied, TiO<sub>2</sub> concentration is the less important one, being more significant its interaction with RH (BD), explained in Section 3.4.

### 3.3.3. Effect of flow rate

The influence of the flow rate on the degradation of 2-propanol is shown in Fig. 5c. Flow rate is an essential factor for the PCO of 2-propanol but in a lesser extent than the RH. The flow rate affects the photocatalytic reaction by changing the convective mass transfer and residence time in the reactor. We note that increasing the flow rate from 100 to 250 mL min<sup>-1</sup> leads to an increase of the mineralization from 74% to 80%. Then, the mineralization decreases from 80% to 59% with the increases of flow rate to 500 mL min<sup>-1</sup>. It is well known that the flow rate has dual effects on the photocatalytic reaction. The increased flow rate improves the photocatalytic reaction by increasing diffusion between VOC and TiO<sub>2</sub> catalyst [28]. The opposite effect observed is the reduction of the residence time which leads to less mineralization of 2-propanol by affecting the adsorption on the surface of TiO<sub>2</sub> and the photocatalytic reaction. It seems, in our study, that the effect of the reduction of the residence time is more predominant than the improvement of mass transfer by diffusion this could be related to the use of cross flow in the reaction system.

### 3.3.4. Effect of relative humidity

Fig. 5d shows us that the effect of RH is related to a significant quadratic effect. The maximum of mineralization corresponds to 0% of RH and during RH enhancement the percentage of mineralization is always decreasing. Increasing the RH from 0% to 60% resulted in a dramatic decrease on the mineralization of 2-propanol from 96% to 32%, indicating that the treatment efficiency for the 2-propanol is a strong function of the water vapour present during the PCO process, this effect is related to the low concentration of the pollutant compared to water concentration.

Relative humidity represents one of the most important parameters for PCO in the gas phase. The impact of humidity has been reported on the efficiency in the air treatment [29]. It was also reported that in the absence of water vapour, the PCO of some VOCs were seriously retarded [30–32] and with high percentages of water vapour on the catalyst surface there is an inhibition in reaction rate because of the effect of the competition adsorption between water vapour and pollutant [33]. Some studies proved that the presence of water also affects the generation of PCO by-products [34]. Authors showed that there is an optimal concentration of water vapour to get the maximal PCO reaction rate [35].

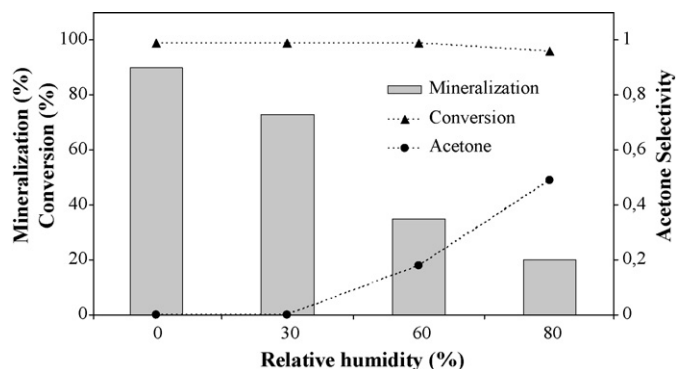


Fig. 6. Effect of different relative humidity percentages on the mineralization, conversion and acetone selectivity from the PCO of 2-propanol (flow rate 100 mL min<sup>-1</sup>, inlet [2-propanol] 700 ppbv, TiO<sub>2</sub> 20 g m<sup>-2</sup>).

More experiments were carried out to better understand the importance of relative humidity on 2-propanol oxidation. Experiments were performed at 100 mL min<sup>-1</sup> flow rate and using different humidity percentages. Main results are summarized in Fig. 6. This figure shows that, whatever the humidity percentages, the presence of humidity is always detrimental. High percentage of mineralization is obtained at RH < 1% [36]. The conversion of 2-propanol was also measured and in all cases values higher than 97% were obtained.

Acetone was detected only at 60% and 80% of RH with a selectivity of 0.18 and 0.49 from the 2-propanol conversion. Because the TiO<sub>2</sub> surface is extremely hydrophilic, almost all the surface adsorption sites of TiO<sub>2</sub> are occupied by water molecules in the presence of humidity. Since water and 2-propanol were adsorbed on the same adsorption sites [37], a competitive interaction was anticipated.

### 3.4. Factors interactions

In addition to the effect of each of the variables such as inlet [2-propanol], flow rate, TiO<sub>2</sub> loading and RH on the mineralization of 2-propanol individually, it is also important to check the interaction effects of these variables, especially two-factor interaction effects. In these graphs, one factor was fixed in its low (–1) and high (+1) level while the other was investigated. These interactions were constructed by plotting both variables together on the same graph and are shown in Fig. 7.

In Fig. 7a, the two-factor interaction of relative humidity and TiO<sub>2</sub> loading was investigated, this interaction (BD) shows us the real importance of TiO<sub>2</sub> loading for the mineralization of 2-propanol. The inlet [2-propanol] and the flow rate were fixed at 400 ppbv and 300 mL min<sup>-1</sup>, respectively. As shown in this figure in dry air (RH < 1%), high values of mineralization (>90%) were observed at different TiO<sub>2</sub> loadings. However there is a significant decrease in mineralization in the presence of humidity especially at low TiO<sub>2</sub> loading (5 g m<sup>-2</sup>), obtaining high percentages of mineralization at different RH always at the high value of TiO<sub>2</sub> loading (20 g m<sup>-2</sup>). This figure shows that the optimal amount of TiO<sub>2</sub> to achieve the maximum of mineralization of 2-propanol depends on the level of RH during the process. The strong interaction between the relative humidity and the TiO<sub>2</sub> concentration (BD) indicates an important interdependence in the response of mineralization.

In Fig. 7b we can note the evaluation of the interactions between flow rate and inlet [2-propanol] in the presence of RH = 30% and 13 g m<sup>-2</sup> TiO<sub>2</sub> loading. The maximum values of mineralization were observed (84–78%) at low 2-propanol concentration (100 ppbv) for the different values of flow rate

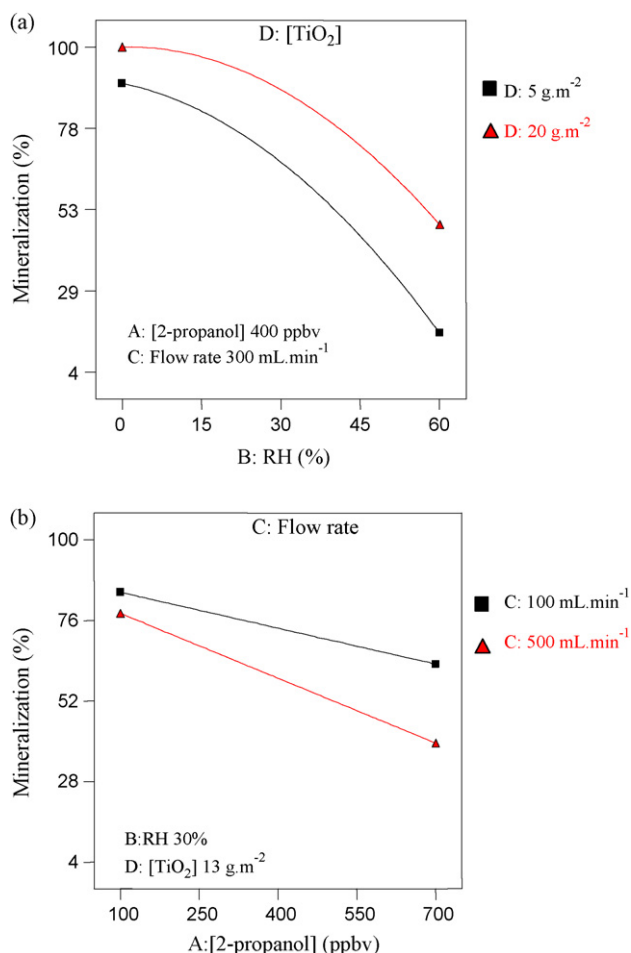


**Fig. 7.** Graphical presentation of the statistical evaluation of the interactions of two factors on the mineralization of 2-propanol. (a) Relative humidity– $[TiO_2]$  and (b) inlet [2-propanol]–flow rate.

( $100\text{--}500 \text{ mL min}^{-1}$ ). The increasing value of the inlet [2-propanol] causes a gradually decreasing of mineralization for both levels of flow rates. The decrease in the percentage of mineralization can be attributed to the fact that the competitive adsorption between water vapour and 2-propanol becomes more important with the increase of the inlet concentration of 2-propanol, causing a negative effect in the mineralization especially at high levels of flow rate. The same interaction studied (2-propanol–flow rate) at dry air (RH < 1%) shows an less important effect of the increasing concentration of 2-propanol (fig. not showed).

### 3.5. Response surface and contour plots for the PCO treatment of 2-propanol based on the mineralization efficiency

We used the statistical software to construct the three-dimensional (3D) response surface and two-dimensional (2D) contour plots of the model-predicted response. These are graphical representations of the regression equation used to determine the optimum values of the variables within the ranges considered. The main target is to hunt efficiently for the optimum values of the variables in such a way that the response is maximized [23]. The contour diagram plot has an infinite number of combinations based on two variables kept at constant and the others varying within the experimental ranges.

Fig. 8 shows the effect of inlet 2-propanol concentration and relative humidity. This figure presents the contour (a) and the

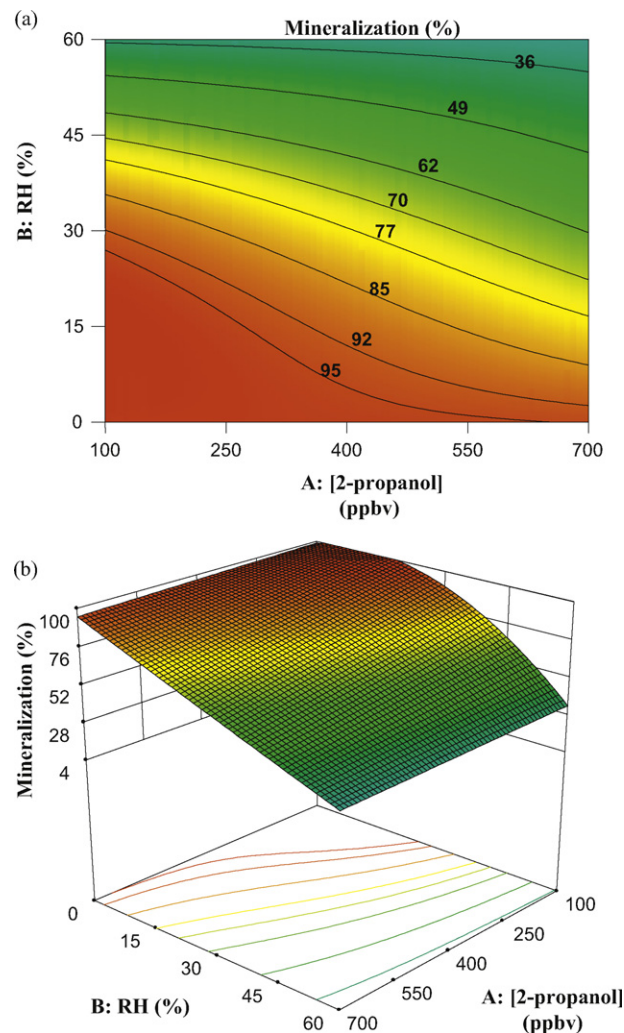


**Fig. 8.** Response surface and contour-lines plots for inlet 2-propanol concentration and relative humidity variables, holding the others variables at they center levels, flow rate  $300 \text{ mL min}^{-1}$  and  $[TiO_2] 13 \text{ g m}^{-2}$ .

response surface (b) plots as an estimate of percent of mineralization as a function of two parameters: inlet 2-propanol concentration and relative humidity (flow rate =  $300 \text{ mL min}^{-1}$ ;  $[TiO_2] = 13 \text{ g m}^{-2}$ ). As it can be understood from this figure, the highest percent of mineralization occurred when both of the independent parameters, inlet [2-propanol] and RH, were kept in their minimum. A considerable decrease in the mineralization was observed upon elevating the relative humidity at all initial 2-propanol concentrations.

### 3.6. Reaction pathway of PCO of 2-propanol

The mechanism for the PCO of 2-propanol by UV illuminated  $TiO_2$  has been extensively studied [26,27,38–41]. There is an agreement in literature to consider that the main gaseous products in the 2-propanol photocatalytic oxidation by using  $TiO_2$  are acetone,  $CO_2$  and  $H_2O$  [42]. Our results are in agreement with previous works.

During the photodegradation, acetone was regarded as the main intermediate that could be oxidated toward final products,  $CO_2$  and  $H_2O$  [43]. The acetone molecules are originated from photocatalytic dehydrogenation of hydrogen bonded 2-propanol molecules, while chemisorbed 2-propoxy species were preferentially oxidized directly to  $CO_2$ . Therefore it can be concluded that

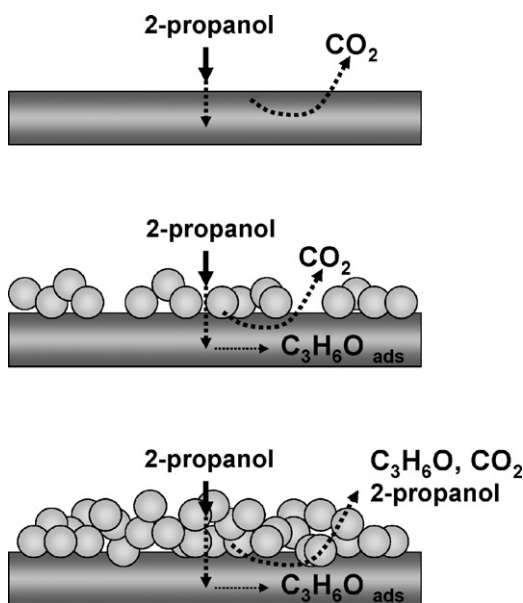


Fig. 9. Schematic proposed for photocatalytic degradation of 2-propanol at indoor air concentrations. (○) H<sub>2</sub>O molecules and (□) TiO<sub>2</sub> support.

the photocatalytic oxidation of 2-propanol on the anatase TiO<sub>2</sub> proceeded along two parallel routes: the oxidation of H-bonded 2-propanol proceeded through intermediates (acetone) and 2-propoxy species should be directly converted to CO<sub>2</sub> [44]. According to our product distribution results of 2-propanol oxidation during the experimental design, the detection of acetone and CO<sub>2</sub> as intermediates in 2-propanol oxidation can support this mechanism. The experiments in the absence of RH shows that the mineralization was nearly 100%, in the experiments with low RH (<30%) the mineralization was lower than 90% and with high levels of RH (>60%) we found low rate of mineralization lower than 35%, acetone and also 2-propanol were detected in the outlet of the reactor. It seems that acetone formed is slowly oxidated to CO<sub>2</sub> and in the presence of high concentrations of water is easily displaced by 2-propanol from the catalyst surface [42]. The scheme represented in Fig. 9 illustrates the pathway for the photocatalytic degradation of 2-propanol observed during the experimental design.

#### 4. Conclusions

It has been demonstrated that the application of the response surface methodology for the optimization of PCO of VOCs can be an interesting alternative to the classical forms of one-variable-at-time in photocatalysis for indoor air studies: (i) in order to better understand the single effects and their interactions of the experimental parameters and (ii) to achieve a high performance of PCO. The high correlation of the model with the experimental results indicates that this analytical procedure can describe any similar photocatalytic system in indoor air treatment. Between all the parameters studied during the experimental design, the results showed the relative humidity as the key factor in the reaction processes. At low RH, high mineralization was found (~90%) without by-products in the gas phase. In contrast, at high RH levels, low levels of mineralization were found because of the competitive adsorption between water vapour and pollutant. Acetone was found as only by-product. The effects of the different parameters,

pollutant conversion and mineralization along with the by-products detection, are the essential information for the evaluation of PCO efficiency and its applications for indoor air quality.

#### References

- [1] J. Mo, Y. Zhang, Q. Xu, J.J. Lamson, R. Zhao, *Atmospheric Environment* 43 (2009) 2229–2246.
- [2] J. Chen, C.-s. Poon, *Building and Environment* 44 (2009) 1899–1906.
- [3] A.T. Hodgson, H. Destailats, D.P. Sullivan, W.J. Fisk, *Indoor Air* 17 (2007) 305–316.
- [4] J.-M. Herrmann, *Catalysis Today* 53 (1999) 115–129.
- [5] J. Zhao, X. Yang, *Building and Environment* 38 (2003) 645–654.
- [6] R.M. Alberci, W.F. Jardim, *Applied Catalysis B: Environmental* 14 (1997) 55–68.
- [7] S. Wang, H.M. Ang, M.O. Tade, *Environment International* 33 (2007) 694–705.
- [8] D.C. Montgomery, *Design and Analysis of Experiments*, 5th ed., John Wiley and Sons, New York, 2001.
- [9] R.H. Myers, D.C. Montgomery, *Response Surface Methodology*, 5th ed., Wiley, New York, 2002.
- [10] A.F. Caliman, C. Cojocaru, A. Antoniadis, I. Poullos, *Journal of Hazardous Materials* 144 (2007) 265–273.
- [11] I.-H. Cho, K.-D. Zoh, *Dyes and Pigments* 75 (2007) 533–543.
- [12] Y. Lin, C. Ferronato, N. Deng, F. Wu, J.-M. Chovelon, *Applied Catalysis B: Environmental* 88 (2009) 32–41.
- [13] H.-L. Liu, Y.-R. Chiou, *Chemical Engineering Journal* 112 (2005) 173–179.
- [14] M.S. Secula, G.D. Suditu, I. Poullos, C. Cojocaru, I. Cretescu, *Chemical Engineering Journal* 141 (2008) 18–26.
- [15] M. Sleiman, D. Vildozo, C. Ferronato, J.-M. Chovelon, *Applied Catalysis B: Environmental* 77 (2007) 1–11.
- [16] J. Mo, Y. Zhang, Q. Xu, Y. Zhu, J.J. Lamson, R. Zhao, *Applied Catalysis B: Environmental* 89 (2009) 570–576.
- [17] T. Tanaka-kagawa, S. Uchiyama, E. Matsushima, A. Sasaki, H. Kobayashi, M. Yagi, M. Tsuno, M. Arai, K. Ikemoto, M. Yamasaki, Y. Otsubo, M. Ando, J. Hideto, H. Tokunaga, *Survey of Volatile Organic Compounds Found in Indoor and Outdoor Air Samples from Japan*, National Institute of Health Sciences, Japan, 2005pp. 27–31.
- [18] P. Wolkoff, G.D. Nielsen, *Atmospheric Environment* 35 (2001) 4407–4417.
- [19] Y. Ohko, A. Fujishima, K. Hashimoto, *The Journal of Physical Chemistry B* 102 (1998) 1724–1729.
- [20] D.S. Forsyth, *Journal of Chromatography A* 1050 (2004) 63–68.
- [21] W.E. Wentworth, K. Sun, D. Zhang, J. Madabushi, S.D. Stearns, *Journal of Chromatography A* 872 (2000) 119–140.
- [22] M.B. Luigi Campanella, Cecilia Costanza, *Annali di Chimica* 95 (2005) 727–740.
- [23] M.A. Bezerra, R.E. Santelli, E.P. Oliveira, L.S. Villar, L.A. Escalera, *Talanta* 76 (2008) 965–977.
- [24] M. Sleiman, P. Conchon, C. Ferronato, J.-M. Chovelon, *Applied Catalysis B: Environmental* 86 (2009) 159–165.
- [25] M. Sleiman, C. Ferronato, J.-M. Chovelon, *Environmental Science & Technology* 42 (2008) 3018–3024.
- [26] W. Xu, D. Raftery, J.S. Francisco, *The Journal of Physical Chemistry B* 107 (2003) 4537–4544.
- [27] C. Chiu-Ping, C. Jong-Nan, L. Ming-Chun, *Journal of Chemical Technology & Biotechnology* 79 (2004) 1293–1300.
- [28] H. Yu, K. Zhang, C. Rossi, *Journal of Photochemistry and Photobiology A: Chemistry* 188 (2007) 65–73.
- [29] N. Bouazza, M.A. Lillo-Ródenas, A. Linares-Solano, *Applied Catalysis B: Environmental* 84 (2008) 691–698.
- [30] A. Bouazza, C. Vallet, A. Laplanche, *Journal of Photochemistry and Photobiology A: Chemistry* 177 (2006) 212–217.
- [31] Y. Luo, D.F. Ollis, *Journal of Catalysis* 163 (1996) 1–11.
- [32] C.H. Ao, S.C. Lee, *Journal of Photochemistry and Photobiology A: Chemistry* 161 (2004) 131–140.
- [33] S.B. Kim, H.T. Hwang, S.C. Hong, *Chemosphere* 48 (2002) 437–444.
- [34] T.N. Obee, *Environmental Science & Technology* 30 (1996) 3578–3584.
- [35] W. Nam, J. Kim, G. Han, *Chemosphere* 47 (2002) 1019–1024.
- [36] G. Marci, E. García-López, L. Palmisano, *Catalysis Today* 144 (2009) 42–47.
- [37] T.N. Obee, R.T. Brown, *Environmental Science & Technology* 29 (1995) 1223–1231.
- [38] Y. Ohko, K. Hashimoto, A. Fujishima, *The Journal of Physical Chemistry A* 101 (1997) 8057–8062.
- [39] M. Addamo, V. Augugliaro, A. Di Paola, E. García-López, V. Loddò, G. Marci, L. Palmisano, *Thin Solid Films* 516 (2008) 3802–3807.
- [40] W. Xu, D. Raftery, *The Journal of Physical Chemistry B* 105 (2001) 4343–4349.
- [41] S.A. Larson, J.A. Widegren, J.L. Falconer, *Journal of Catalysis* 157 (1995) 611–625.
- [42] F. Arsac, D. Bianchi, J.M. Chovelon, C. Ferronato, J.M. Herrmann, *The Journal of Physical Chemistry A* 110 (2006) 4202–4212.
- [43] M.D. Hernández-Alonso, I. Tejedor-Tejedor, J.M. Coronado, M.A. Anderson, J. Soria, *Catalysis Today* 143 (2009) 364–373.
- [44] H. Zhang, H. Yu, A. Zheng, S. Li, W. Shen, F. Deng, *Environmental Science & Technology* 42 (2008) 5316–5321.